

A Study of the Alignment of SDSS DR16 galaxies at REDSHIFT 0.24 to 0.27

Janak Ratna Malla^{1*}Walter Saurer²Binil Aryal³DOI: <https://doi.org/103126/academia.v5i1.89173>¹Amrit campus, Tribhuvan University, Kathmandu, Email: janak.malla@ac.tu.edu.np²Institute of Astro-particle Physics, Innsbruck University, Austria, Email: walter.saurer@uibk.ac.at³Central Department of Physics, Kirtipur, Kathmandu, Email: binil.aryal@cdp.tu.edu.np* Corresponding Author: janak.malla@ac.tu.edu.np

Article History: Received: July. 11, 2025 Revised: Sept. 01, 2025 Received: December 26, 2025

Abstract

We studied the spatial orientation of spin vectors of 1715 SDSS DR16 galaxies within the redshift range of 0.24 to 0.27 using the u-band imaging ($\lambda_{\text{eff}} \approx 355$ nm). This study analyzed a total of 1715 galaxy samples to provide new insights into the formation and evolution of galaxies and help interpret observational data. Adopting Flin & Godlowski method, we transformed the two-dimensional projected images into three-dimensional spin vector components: specifically, polar (θ) and azimuthal (ϕ) angles and studied the angular momentum alignment. Through the four simultaneous tests chi-square, auto-correlation, and Fourier analysis statistical tests, we concluded that the SDSSDR16 data of 1715 galaxies support strong anisotropy in the polar angle distribution and point toward isotropy in the azimuthal angle distribution. These findings support the Hierarchical model of the galaxy evolution theory.

Keywords: Galaxies, SDSS DR16, Isotropy, Anisotropy, U-band, Spatial Orientation

Introduction

The accelerating expansion of our universe is primarily composed of hydrogen and helium, along with a small fraction of heavier elements. By large-scale structures, we refer to the vast clusters of galaxies that are fundamental to understanding the origin, distribution, and evolution of galaxies and the intergalactic medium. Current theory traces these grand patterns back to the relentless gravitational amplification of minute fluctuations seeded in the primordial density field.

Redshift has several components: the primary term from the Hubble expansion of space (cosmological redshift), a smaller line-of-sight term from the galaxy's peculiar velocity relative to the cosmic rest frame (Doppler redshift), and a typically minor shift from photons escaping the host halo's gravitational potential (gravitational redshift). The measured redshift for each galaxy is the relativistic combination of these contributions, which must be considered when calculating comoving distances and the angular diameter relation that connects observed ellipticities to intrinsic spin vectors.

The question of whether galaxy alignment is a genuine astrophysical phenomenon or a statistical artifact has long been a central challenge in cosmology. The definitive empirical framework for this

investigation was established by Godłowski (1993, 1994), his methodology relies on a set of four simultaneous statistical tests. This rigorous approach, anchored by the strict criterion effectively minimizes false positives originating from Poisson noise, ensuring that any detected alignment is a robust signal, not a random fluctuation. Previous applications of this framework to early datasets, such as the CfA (Centre for Astrophysics) redshift survey and the galaxy sample from Aryal & Saurer (2006), consistently yielded null results, suggesting an isotropic distribution of galaxy orientations.

Data Compilation

For this study, we used data from the Sloan Digital Sky Survey (SDSS), specifically from Data Release 16 (DR16). We started by selecting the top 3000 galaxies within a red shift range of $0.24 \leq z \leq 0.27$. After filtering the dataset to eliminate errors and irrelevant entries, the final sample consisted of 1715 galaxies. These galaxies were grouped into different bins to help us study how their spin directions are oriented in space. The data were subsequently processed mathematically to determine the right ascension (RA), declination (DEC), position angle (PA), and inclination angle (IA) for each galaxy as shown in Table 1.

Table 1

Galaxy data with u-band magnitude, coordinates, redshift, and ellipticity measurements

U	RA	DEC	redshift	e1 (me1_ u)	e2 (me2_ u)
20.80604	214.6149	-0.28453	0.249908	0.123343	0.246625
21.96011	215.606	-0.224	0.247797	0.089644	-0.02483
20.9031	215.7473	-0.22749	0.265719	0.030861	0.288352
20.74908	216.2463	-0.27144	0.268639	0.394776	0.466154
21.33534	216.5049	-0.24663	0.254456	-0.36569	-0.26757
21.40398	219.5154	-0.32183	0.246982	-0.21341	0.806738
21.77234	222.39	-0.34408	0.252128	0.427457	0.300072
21.95911	222.4922	-0.33082	0.251155	-0.33736	0.291582
22.12921	227.3475	-0.20609	0.263903	0.728388	-0.65764
22.73461	227.6822	-0.35362	0.262004	-0.41504	0.587761
22.29334	231.3747	-0.2604	0.260234	-0.29579	0.436335
21.17204	233.4151	-0.23769	0.259354	0.117777	0.396547
21.44412	233.3585	-0.38596	0.260598	0.361963	-0.49771
22.18389	239.7927	-0.25831	0.250809	0.016711	0.349118
23.10407	170.7263	0.026196	0.259321	-0.46346	-12.9089
25.08158	185.9861	0.132431	0.263965	-0.02473	-0.28166
20.52574	189.8243	0.112479	0.248062	0.0408	-0.17055
19.62704	190.6699	0.112991	0.257835	0.118779	-0.11884

Similarly, the distributions of right ascension (α), declination angle (δ), position angle (P), and inclination angle (IA) were analyzed for the galaxies in the sample. These distributions are presented in the figure below. The histograms represent the number of observed galaxies.

Table 2

Appropriate binning of RA, DEC, PA, and IA with their observed number (O), and expected number (E). Here, E is the corresponding number of galaxies in 10^6 virtual galaxies created by the computer simulation.

RA	O	E	DEC	O	E	PA	O	E	IA	O	E
10	44	25655.97668	-12.5	8	4664.723032	5	1	583.090379	2.5	12	6997.084548
30	73	42565.59767	-7.5	159	92711.37026	15	8	4664.723032	7.5	67	39067.05539
50	144	83965.01458	-2.5	288	167930.0292	25	16	9329.446064	12.5	87	50728.86297
70	37	21574.34402	2.5	437	254810.4956	35	18	10495.62682	17.5	130	75801.74927

Figure 1

Distribution of RA (α) and Declination (δ) for the galaxies within the sample

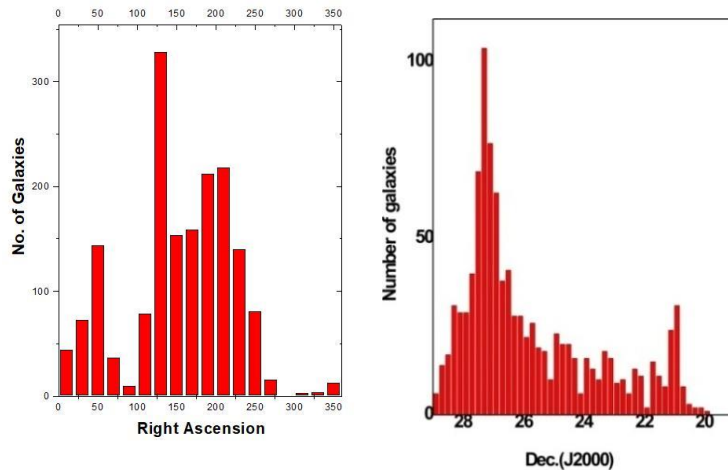
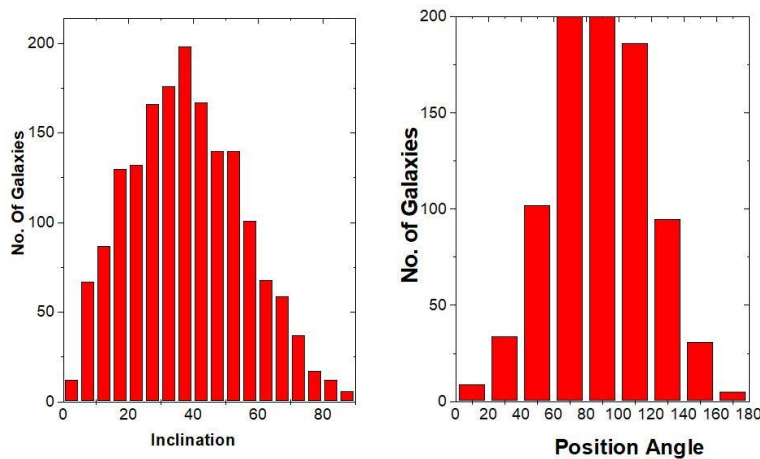


Figure 2

Distribution of inclination angle (IA) and Position angle (PA) for the galaxies within the sample



Methods

The initial data set comprises right ascension, declination, major axis, minor axis, and position angle, all measured in two dimensions. However, a three-dimensional description is required to determine the spin-vector orientation. To convert this 2-D information into 3-D, the position-angle-inclination (PA-inclination) method of Flin and Godłowski is applied. The transformation is performed using the following equations:

$$\sin\theta = -\cos i \sin\alpha \pm \sin i \sin p \cos\delta \tag{1}$$

$$\sin\varphi = (\cos\theta)^{-1}[-\cos i \cos\delta \sin\alpha + \sin i (\mp \sin p \sin\delta \sin\alpha \mp \cos p \cos\alpha)] \tag{2}$$

where, i is the inclination angle, δ is declination angle, α is right ascension angle and p is position angle.

By using Holmberg's formula (1946) inclination angle is calculated.

$$\cos^2 i = \frac{\left(\frac{b}{a}\right)^2 - q^{*2}}{1 - q^{*2}} \tag{3}$$

Where, b/a is the axial ratio and q^* is the intrinsic flatness of the galaxy. We utilized the value of $q^*=0.2$ in our computation. The inclination angle is negative for galaxies with an axial ratio less than 0.2. As a result, we only include 1715 galaxies in our paper.

Results and Discussion

Figure 3 and Figure 4 show the all-sky distribution of 1715 galaxies in the 3D plane and the corresponding contour map, respectively. Strong clustering is evident at right ascension between 150° and 250° and redshift between 0.255° and 0.265° , suggesting the presence of a filament or sheet-like overdensity in this redshift slice. The low-density wings at the RA extremes indicate that the galaxies are not uniformly distributed across the sky. These concentrated regions of galaxies within a relatively confined space can be considered substructures, potentially forming larger galaxy clusters.

Figure 3

3D scattering showcasing the distribution of 1715 SDSSDR16 galaxies in the sky

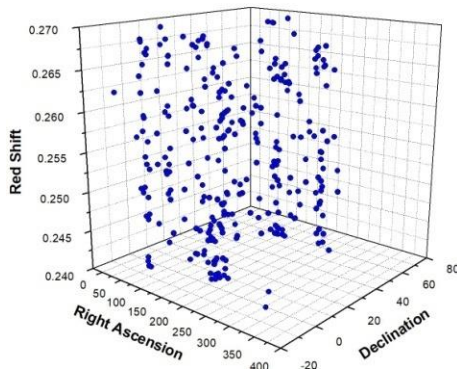
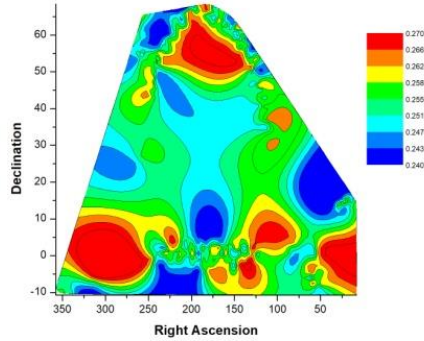


Figure 4

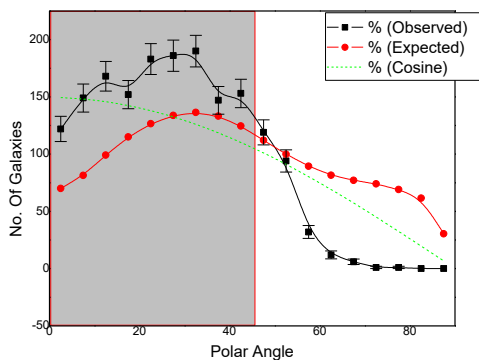
Contour map illustrating the spatial distribution of 1715 SDSSDR16 galaxies across the sky



This study utilizes a sample comprising 1715 galaxies, each yielding two potential values for the polar angle (θ) and the azimuthal angle (ϕ), resulting in a total of 3430 angle solutions. The analysis focuses exclusively on the absolute values of θ , with the distributions of the polar and azimuthal angles examined independently. Figure 5 shows the distribution of the polar angle (θ), while Figure 6 illustrates the distribution of the azimuthal angle (ϕ) for all galaxies in the dataset.

Figure 5

The polar angle (θ) distribution of 1715 SDSSDR16 galaxies. The solid line symbolizes the expected anisotropic distributions. The dashed lines symbolize the cosine distributions. The observed distribution is symbolized by solid circles with $\pm 1\sigma$ error bars.

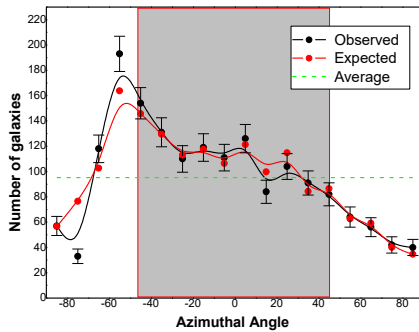


In the shaded region ($\theta < 45^\circ$), prominent humps centered at $\theta \approx 27^\circ$ elevate the observed counts to ~ 190 galaxies, about 50% above the smooth cosine expectation (~ 125). This excess indicates a marked preference for spin vectors aligned nearly parallel to the equatorial plane. Conversely, in the unshaded region ($\theta > 45^\circ$), a pronounced dip centered at $\theta \approx 57^\circ$ drops the observed counts to ~ 70 galaxies, roughly 45% below the expected level, revealing a striking deficit of galaxies whose spins are oriented perpendicular to the equatorial plane.

The deviation from both the expected and cosine curves, particularly at higher θ , reinforces the presence of anisotropy in the polar angle distribution.

Figure 6

Distribution of the azimuthal angle (ϕ) for 1715 SDSSDR16 galaxies. The solid line represents the theoretical isotropic distribution, while the dashed lines denote the mean observed distributions. The data points, shown as solid circles with $\pm 1\sigma$ error bars, correspond to the measured distribution.



For the azimuthal angle, a slight peak near $\phi \approx 0^\circ$ increases the galaxy count to about 205, while a gentle dip near $\phi \approx \pm 50^\circ$ reduces it to roughly 175. Both of these deviations fall within the $\pm 1\sigma$ range of the expected mean (~ 190), indicating no statistically significant directional preference. In contrast, the clear excesses and deficits observed in the polar-angle distribution, together with the azimuthal pattern as consistency with isotropy, reveal a pronounced anisotropy in θ but isotropy in ϕ , highlighting the influence of large-scale cosmic structures or environmental torques on galaxy spin alignments at this redshift.

Table 3

Statistical analysis of the polar (θ) and azimuthal (ϕ) angle distributions in SDSS DR16 galaxy sample

Statistics	Polar angle(θ)	Azimuthal angle (ϕ)
$P(>\chi^2)$	0.00	0.00
$C/C(\sigma)$	129.92	-0.62
$\Delta_{11}/\sigma(\Delta_{11})$	23.52	0.10
$P(>\Delta_1)$	0.00	0.04

The statistics of the polar (θ) and azimuthal (ϕ) angle distributions of 1715 SDSS DR16 galaxies are displayed in Table 1. In this sample, the statistical analysis of the polar angle distribution reveals a chi-square probability, $P(>\chi^2)$, of approximately 0. Such an exceedingly small probability value provides compelling evidence of a statistically significant departure from isotropy.

The auto-correlation coefficient $C/\sigma(C)$ is found to be 129.92, which is significantly greater than the 1σ threshold, indicating a high degree of non-randomness and strong correlation in the distribution of

polar angles. This suggests a pattern or alignment in the orientation of spin vectors rather than a random (isotropic) distribution.

Furthermore, the first-order Fourier coefficient, Δ_{11}/σ (Δ_{11}), is computed to be 23.52, which greatly exceeds the 1.5σ limit, confirming a statistically significant deviation from isotropy. The corresponding first-order Fourier probability $P(> \Delta_1)$ is extremely low, with a value of 0.00, further reinforcing the presence of anisotropy. These combined statistical measures: chi-square, auto-correlation, and Fourier analysis, strongly suggest that the spatial orientation of galaxy spin vectors in terms of polar angles is anisotropic. The positive sign of the first-order Fourier coefficient indicates a tendency for galaxy spin vectors to be aligned predominantly along the equatorial coordinate system.

For the azimuthal angle distribution, the chi-square probability $P(> \chi^2)$ is calculated to be 0.00, falling below the 5% significance threshold. This result indicates a statistically significant deviation from isotropy according to the chi-square test. However, other important statistical test shows strong isotropy. The auto-correlation coefficient $C/\sigma(C)$ is obtained to be -0.62, which is far below the 1σ level, indicating a weak correlation that indicates strong isotropy.

Moreover, the first-order Fourier coefficient, $\Delta_{11}/\sigma(\Delta_{11})$, is found to be 0.10, which is below the standard 1.5σ threshold, suggesting a preferential isotropy in the ϕ -distribution. The corresponding Fourier probability $P(> \Delta_1)$ is 0.04, which is less than the 0.15 cutoff, again indicating mild deviation from isotropy.

Although the chi-square test indicates anisotropy and the first-order Fourier coefficient suggests mild anisotropy, the auto correlation and first-order Fourier tests clearly indicate strong and significant isotropy in the azimuthal angle distribution. Also, when we convert the first-order Fourier coefficient $P(> \Delta_1)$ which is in upper tail probability in to lower tail probability $P(< \Delta_1)$, we see that $P(< \Delta_1)$ is much more greater than 0.15. Thus, therefore the fourth simultaneous test fails even though the first three indicators surpass their individual thresholds. Consequently, the results obtained from the sample are judged to be consistent with isotropy under the adopted criteria.

To sum up, the statistical findings indicate anisotropy within the polar angle distribution while demonstrating pronounced isotropy in the azimuthal angle distribution. These findings reinforce the graphical interpretations discussed earlier and suggest the presence of large-scale or environmental influences on the spin vector orientations of galaxies at the examined redshift range.

Conclusion

In this paper, we explored the alignment of spin vectors for galaxies from the SDSSDR16 dataset, selecting those within the redshift range $0.24 \leq z \leq 0.27$ using u-band photometric data.

The outcomes of these statistical evaluations for the polar-angle distribution reveal clear evidence of strong anisotropy. The extremely low chi-square probability $P(> \chi^2)$, the high auto-correlation ratio $C/\sigma(C)$, and the large first-order Fourier coefficient $\Delta_{11}/\sigma(\Delta_{11})$ with extremely low corresponding probability $P(> \Delta_1)$ collectively indicate that galaxy spin vectors are not randomly distributed but instead

exhibit a strong tendency to align parallel to the equatorial coordinate system. By contrast, the azimuthal-angle distribution is largely consistent with isotropy.

But this anisotropy in polar test and isotropy in azimuthal test can signify several physical phenomenon behind this result. Large-scale tidal torques from filaments preferentially align spin vectors toward the radial (polar) direction and Azimuthal orientations lack a persistent external torque axis, leaving spins randomly distributed. The presence of humps and dips in the angular distributions further supports the role of local and global influences on galactic spin vector orientation.

References

- Aryal, B., & Saurer, W. (2000). Comments on the expected isotropic distribution curves in galaxy orientation studies. *Astronomy and Astrophysics*, 364, L97–L100.
- Aryal, B., & Saurer, W. (2001). The influence of selection effects on the isotropic distribution curve in galaxy orientation studies. In *Galaxy disks and disk galaxies* (Vol. 230, pp. 145–146).
- Aryal, B., & Saurer, W. (2004). Spin vector orientations of galaxies in eight Abell clusters of BM type I. *Astronomy & Astrophysics*, 425(3), 871–879.
- Aryal, B., & Saurer, W. (2006). Spatial orientations of galaxies in 10 Abell clusters of BM type II–III. *Monthly Notices of the Royal Astronomical Society*, 366(2), 438–448.
- Aryal, B., Paudel, S., & Saurer, W. (2007). Spatial orientations of galaxies in seven Abell clusters of BM type II. *Monthly Notices of the Royal Astronomical Society*, 379(3), 1011–1021.
- Blumenthal, G. R., Faber, S. M., Primack, J. R., & Rees, M. J. (1984). Formation of galaxies and large-scale structure with cold dark matter. *Nature*, 311(5986), 517–525.
- Codis, S., Pichon, C., Devriendt, J., Slyz, A., Pogosyan, D., Dubois, Y., & Sousbie, T. (2018). Alignment of galaxy spins in the cosmic web. *Monthly Notices of the Royal Astronomical Society*, 477, 4192–4211. <https://academic.oup.com/mnras/article-abstract/477/4/4192/4938668>
- Doroshkevich, A. G. (1970). Spatial structure of perturbations and the origin of rotation of galaxies in the theory of fluctuation. *Astrophysics*, 6, 320–331. <https://link.springer.com/article/10.1007/BF01001637>
- Doroshkevich, A. G. (1973). The orientation of rotation of galaxies. *Astrophysical Letters*, 14, 11–13.
- Doroshkevich, A. G., & Shandarin, S. F. (1978). Spatial structure of protoclusters and the formation of galaxies. *Monthly Notices of the Royal Astronomical Society*, 184, 643–660.
- Flin, P., & Godlowski, W. (1986). The orientation of galaxy groups and formation of the local supercluster. *Monthly Notices of the Royal Astronomical Society*, 222, 525.
- Gamow, G. (1952). The role of turbulence in the evolution of the universe. *Physical Review*, 86, 251.
- Gamow, G., & Teller, E. (1939). On the origin of great nebulae. *Physical Review*, 55, 654.
- Godlowski, W. (1993). Galactic orientation within the local supercluster. *Monthly Notices of the Royal Astronomical Society*, 265, 874–880.
- Godlowski, W. (1994). Some aspects of the galactic orientation within the local supercluster. *Monthly Notices of the Royal Astronomical Society*, 271, 19–30.
- Godlowski, W. (2011). Some observational aspects of the orientation of galaxies [Preprint]. arXiv:1111.1777

- Guth, A. H. (1981). Inflationary universe: A possible solution to the horizon and flatness problems. *Physical Review D*, 23(2), 347–356.
- Hahn, F. (n.d.). SDSS telescope [Photograph]. Sloan Digital Sky Survey. <https://www.symmetrymagazine.org/article/february-2015/>
- Hawking, S., & Ellis, G. (1973). *The large scale structure of space-time*. Cambridge University Press.
- Hawley, D., & Peebles, P. (1975). Distribution of observed orientations of galaxies. *The Astronomical Journal*, 80, 477–491.
- Heidmann, J., Heidmann, N., & de Vaucouleurs, G. (1972). Inclination and absorption effects on the apparent diameters, optical luminosities and neutral hydrogen radiation of galaxies-III. Theory and applications. *Memoirs of the Royal Astronomical Society*, 75, 121.
- Holmberg, E. (1946). On the apparent diameters and the orientation in space of extragalactic nebulae. *Meddelanden från Lunds Astronomiska Observatorium Serie II*, 117, 3–82.
- Hu, W. (1999). Power spectrum tomography with weak lensing. *The Astrophysical Journal Letters*, 522(1), L21.
- Jaaniste, J., Saar, E., Longair, M. S., & Einasto, J. (Eds.). (1978). *The large scale structure of the universe: Proceedings of IAU Symposium 79* (p. 448).
- Kashikawa, N., & Okamura, S. (1992). Spatial orientation of spin vectors of galaxies in the local supercluster. *Publications of the Astronomical Society of Japan*, 44, 493–507.
- Kessler, R. (2011). SDSS [Webpage]. <https://kicp.uchicago.edu/research/projects/sdss.html>
- Kitzbichler, M., & Saurer, W. (2003). Investigation of galaxy orientations in the Coma cluster. *Astronomische Nachrichten*, 324(2), 94.
- Malla, J., Aryal, B., & Saurer, W. (2019). No preferred alignments of angular momentum vectors of galaxies in the SDSS supercluster S [202-001+0084]. *Proceedings of the International Astronomical Union*, 14(S353), 259–261.
- Malla, J. R., Saurer, W., & Aryal, B. (2020). Spatial orientation of galaxies in the supercluster S[227+006+0078]. *Bibechana*, 17, 117–122.
- Malla, J. R., Saurer, W., & Aryal, B. (2022). Spatial orientation of galaxies in the substructures of SDSS supercluster S[184+003+0077]. *Bulgarian Astronomical Journal*, 37, 97.
- Ozernoy, L. M. (1974). Whirl theory of the origin of galaxies and clusters of galaxies. In *Symposium-International Astronomical Union* (Vol. 63, pp. 227–240). Cambridge University Press.
- Ozernoy, L. M., Longair, M. S., & Einasto, J. (1978). Large scale structure of the universe. *IAU Symposium*, 79, 409.
- Peebles, P. J. E. (1969). Origin of the angular momentum of galaxies. *The Astrophysical Journal*, 155, 393.
- Stein, R. (1974). Galaxy formation from primordial turbulence. *Astronomy & Astrophysics*, 35, 17–29.
- von Weizsäcker, C. (1951). The evolution of galaxies and stars. *The Astrophysical Journal*, 114, 165.
- Yadav, S. N., Aryal, B., & Saurer, W. (2017). Preferred alignments of angular momentum vectors of six galaxies in six dynamically unstable Abell clusters. *Research in Astronomy and Astrophysics*, 17, 7.
- York, D. G., Adelman, J., Anderson, J. E., Anderson, S. F., Annis, J., Bahcall, N. A., et al. (2000). The Sloan Digital Sky Survey: Technical summary. *The Astronomical Journal*, 120, 1579–1587.
- York, D.G., Adelman, J., Anderson J.E., Anderson, Scott F., Annis, James, Bahcall, Neta A. et al. (2000). The Sloan Digital Sky Survey: Technical Summary. *The Astronomical journal*, 120, 1579-1587.